Modeling the Elastic Energy of Alloys: Potential Pitfalls of Continuum Treatments

Arvind Baskaran,[1] Christian Ratsch,[2] and Peter Smereka*[3]

[1]*Department of Mathematics, University of California, Irvine, CA 92697-3875.*†
[2]*Department of Mathematics and Institute for Pure and Applied Mathematics, University of California, Los Angeles, CA*‡
[3]*Department of Mathematics and Michigan Center for Theoretical Physics, University of Michigan, Ann Arbor, MI 48109.*§

arXiv:1410.5472v2 [cond-mat.mtrl-sci] 4 Nov 2015

Some issues that arise when modeling elastic energy for binary alloys are discussed within the context of a Keating model and density functional calculations. The Keating model is a simplified atomistic formulation based on modeling elastic interactions of a binary alloy with harmonic springs whose equilibrium length is species dependent. It is demonstrated that the continuum limit for the strain field are the usual equations of linear elasticity for alloys and that they correctly capture the coarse-grained behavior of the displacement field. In addition, it is established that Euler-Lagrange equation of the continuum limit of the elastic energy will yield the same strain field equation. This is the same energy functional that is often used to model elastic effects in binary alloys. However, a direct calculation of the elastic energy atomistic model reveals that the continuum expression for the elastic energy is both qualitatively and quantitatively incorrect. This is because it does not take atomistic scale compositional non-uniformity into account. Importantly, this result also shows that finely mixed alloys tend to have more elastic energy than segregated systems, which is the exact opposite of predictions made by some continuum theories. It is also shown that for strained thin films the traditionally used effective misfit for alloys systematically underestimate the strain energy. In some models, this drawback is handled by including an elastic contribution to the enthalpy of mixing which is characterized in terms of the continuum concentration. The direct calculation of the atomistic model reveals that this approach suffers serious difficulties. It is demonstrated that elastic contribution to the enthalpy of mixing is non-isotropic and scale dependent. It is also shown that such effects are present in density-functional theory calculations for the Si/Ge system. This work demonstrates that it is critical to include the microscopic arrangements in any elastic model to achieve even qualitatively correct behavior.

I. INTRODUCTION

Many modern material systems consist of alloys of two or more species. Applications of such alloy systems include semiconductor systems for new optoelectronic devices [1], oxides for optical and electronic applications [2], hydrogen storage systems [3], and more. Different species typically have different lattice constants leading to elastic strain, which can significantly impact the performance and stability. Of particular interest is the strain driven formation and self-organization of heterostructures such as quantum dots for semiconductor systems [4–7]. It is therefore of paramount importance to develop models that properly describe the effect of strain in alloy systems.

The challenge in modeling alloys is that the total energy of an alloy system depends on the composition. This compositional dependence is hard to characterize and a common approach is to assume a species dependent bond lengths and bond energies. This allows one to separate the total energy into the chemical and elastic parts. The alternative is to work with just the total energy. This is usually not tractable and the separation allows one to construct tractable models. In the case of alloys of lattice mismatched elements, the difference in lattice spacing introduces compositionally dependent strain. This is not simply characterized by modeling the response of the material to applied stress. These alloys retain a stress free strain. This strain is determined as the deviation of the bond lengths from their equilibrium values. However, if the bond lengths in the bulk are environmentally dependent, it would not be possible to decompose the energy into chemical and

* Deceased
†Electronic address: baskaran@math.uci.edu
‡Electronic address: cratsch@ipam.ucla.edu
§Electronic address: psmereka@umich.edu

elastic parts. Fortunately an environmentally independent bond length appears to be a reasonable approach to modeling microscopic strain in alloys (see Tsao [8] page 94).

In this paper we revisit the issue of modeling of elastic energy of a binary alloy. The models for elastic energy of alloys fall under two broad categories, namely continuum models and discrete/atomistic models. Reality being that alloys are made of discrete atoms, a fully atomistic description would be the model of choice. However, for practical reasons continuum models are often preferred.

Continuum models aim to characterize the alloy in terms of macroscopic quantities. These macroscopic quantities must vary slowly on the atomistic scale for a continuum model to be consistent. For an alloy, the concentration field does not in general vary slowly on the atomistic scale. However, one can introduce an average concentration which can be constructed to vary smoothly on atomistic scales. It is apparent that for alloys one can make good predictions of coarse-grained displacement fields using continuum theory.

However, the issue of deducing the elastic energy using continuum theory is more difficult. A common starting point is to choose the reference lattice for the alloy in accordance to Vegard's law based on the average concentration. Vegard's law states that the average lattice spacing of an alloy varies linearly with concentration (see [8]). A second but more important assumption is that the stress free strain of a uniform alloy in this reference state is zero. Under these assumptions, it can be shown [9, 10] that for a nonuniform isotropic alloy the elastic energy can be written as

$$W_C = \frac{\eta^2 E}{1-\nu} \int_V (\theta - \theta_0)^2 dV. \tag{1}$$

In Eq. (1), η is the effective misfit, E is Young's modulus, ν is the Poisson ratio, θ is the composition field of the alloy and θ_0 is its average. This formulation has been used to study a wide range of problems including strain driven morphological instabilities, spinodal decomposition, segregation and microstructure evolution in metal and semiconductor alloys [5–7, 10, 11]. The formula given by Eq. (1) implies that non-uniformity of the alloy will result in an increase in elastic energy. For this reason, it is often suggested that contributions to the free energy that arise from atomistic misfit stabilize an alloy or equivalently that intermixing will lower the elastic energy of the alloy.

While Vegard's law in itself is known to be true for some systems [12, 13], it is a statement about the average lattice spacing of alloys. In particular it does not exclude the existence of microscopic stress free strain with respect to the reference lattice. Using a Keating model it has been argued (e.g. Tsao [8]) that for alloys there is microscopic strain even when the alloy atoms are placed in a lattice given by Vegard's law. Thus, the stress free strain is not zero even when the composition appears to be macroscopically uniform. The energy stored in the springs has been used as an estimate for the contribution to the elastic energy due to this microscopic strain (e.g. Tsao [8]). The strain energy associated with this microscopic strain can be considered the elastic contribution to the enthalpy of mixing, H. Then one could posit (e.g. de Fontaine [14] or Ren et al [15]) that the total elastic energy of the alloy can be written as

$$W = W_C + H. \tag{2}$$

The atomistic scales are captured by H whereas W_C is used for the continuum scales. This is only true in the presence of a clear separation of scales. In many time dependent problems there is a range of scales, especially as the system coarsens. For example, in a finely mixed alloy the dominant contribution will come from H, while the microscopic strain energy will lessen in favor of W_C as the alloy coarsens. In fact, we will present results that suggest that the total elastic energy, $W_C + H$, can actually decrease as the system coarsens. Importantly, this means that elastic interactions that arise from atomistic misfit can destabilize an alloy; in other words, they will enhance segregation.

We are not the first to consider some of the issues discussed here. For example, Eshelby [16] argued that for materials whose internal energy is elastic in origin the disordered state is unstable. On the other hand, from Cahn [9] it would seem that the disordered state is stable. De Fontaine [14] calls this the Elastic Energy Paradox. This paradox has also been observed by Cook and de Fontaine [17] and Khachaturyan [18] (see Chapter 13). The physical origin of both the continuum elastic energy and the atomistic elastic enthalpy is the same: different atomistic sizes of the alloy species. We shall see that the source of confusion is in treating them separately. They are both elastic energies, but they are operating on different length scales.

There is some experimental evidence that atomistic misfit will destabilize alloys. In the case of thin film growth of a Si-Ge alloy on Si, Cullis et al [19] present experimental evidence that lateral

segregation occurs to lower strain. In metallurgy, Hume-Rothery, Mabbott and Evans [20], based on experimental observations, proposed the "15% rule" which states that binary solid solutions are very difficult to form if the atomic size factor exceeds ~ 15 %. Eshelby [16] asserted that this rule was a consequence of elastic instability of the disordered state. In related work, King [21] suggests that certain alloys based on copper are unstable due to atomistic size effects. Furthermore, Woodilla and Averbach [22] report that the critical temperature for spinodal decomposition in experiments with Au-Ni is $\sim 220°$, whereas Golding and Moss [23] used Cahn's approach and predicted it to be $\sim 0°$ C. Ren et al [15] surmise that if the enthalpy term was included it would raise this prediction to more closely match experimental observations.

In this paper, we start with a well known atomistic model for a binary alloy in which the bond energy is based on harmonic springs connecting atoms. The atoms are placed on a simple square lattice with springs connecting nearest and next to nearest neighbors with the equilibrium lengths being species dependent. First, we derive the discrete equations for the displacement field and establish that if one coarse-grains these equations one will recover the usual continuum equations of elasticity. This calculation reveals that continuum theory does a good job at predicting average strain fields. Based on the form of the discrete elastic energy one can propose a continuum version of the elastic energy and recover a well known and well used elastic energy which we will denote W_C. Furthermore, we establish that the Euler-Lagrange equations associated with W_C yield the continuum equations that were derived from coarse-graining the atomistic equations. In addition, if we consider the case where continuum equations are isotropic, the elastic energy of our alloy takes the same form as (1).

However, a direct calculation of the elastic energy of the atomistic model in mechanical equilibrium reveals that its behavior can be quite different from its continuum counterpart and the key results of this paper are the following:

1. This calculation demonstrates that the elastic energy is anisotropic and scale dependent. Indeed, the calculation shows that in order to evaluate the elastic energy one needs to understand the behavior of the concentration field on all scales ranging from the atomistic to the continuum. The calculation shows that expressions like Eq. (1) can only be valid when the system is almost completely segregated.

2. Furthermore, it also shows that the elastic energy can be changed by rearrangements at the atomistic scale that would not affect the continuum concentration field. Segregation at the atomistic scale can lower the elastic energy and segregation is preferred over intermixing if one accounts for the atomistic scale details. This is not captured by the continuum theory which not only does not distinguish between the different configurations with microscopic segregation (due to lack of resolution) but in fact predicts the opposite.

3. Our work demonstrates that it is critical to include the microscopic arrangements in any elastic model to achieve even qualitatively correct behavior. Specifically, we show that the enthalpy of mixing H depends both on the direction and wavenumber of the alloy's compositional variations. It is important to note that lack of microscopic information is a direct consequence of the assumption that the stress free strain in the reference lattice is zero. We demonstrate that even though the average stress free strain in the reference lattice is zero the strain energy is not.

Interestingly, in the modeling of heteroepitaxial growth inclusion of any sort of elastic contribution to the enthalpy of mixing is largely ignored (e.g. Spencer et al [5] or Shenoy et al [7]). For models of spinodal decomposition (e.g. Cahn [9]) the enthalpy of mixing that includes the microscopic strain is not explicitly included but it can be argued that it is implicitly included in the free energy term (see the discussion in the footnote on page 1478 of Ref. [10]). Even when enthalpy of mixing is included it is assumed to be a function of the macroscopic concentration field (i.e, $H = H(\theta)$). However, in view of our discrete calculation it follows that H must depend on the atomistic details of the alloy and among other things must be scale dependent.

Our calculations below are based on a ball and spring model but we surmise that they are valid for real materials as well. To provide justification of this assertion we also present calculations using density-functional theory applied to periodic Si/Ge. For example, we consider three dimensional checker-board patterns with cubes of Si alternated with cubes of Ge in which the size of the cubes is varied. The calculations show that as the sizes of the cubes are increased the elastic energy is reduced - in agreement with the ball and spring model. Other arrangements of alloys were also

considered and these also make it clear that the elastic energy will depend on the atomistic details of the alloy.

II. ATOMISTIC ALLOY MODEL

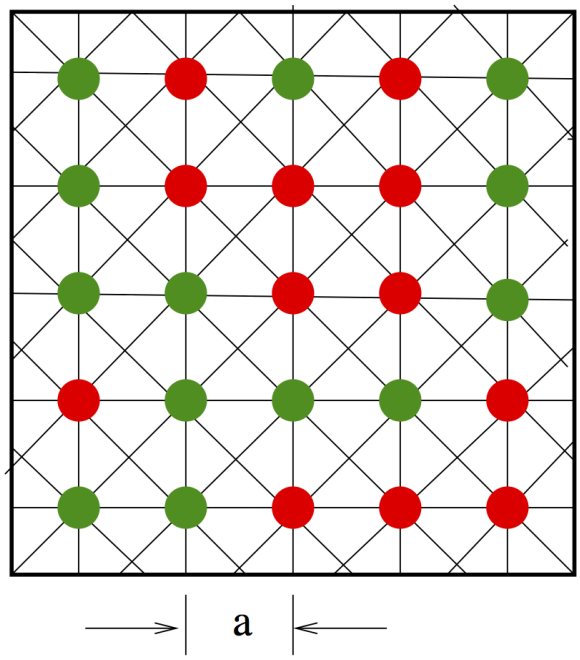

FIG. 1: (Color Online) The schematic of the ball and spring model when the atom are located on the reference configuration

We consider a binary alloy with lattice mismatch (say Si/Ge for ease of exposition) and use a ball spring model on a simple square lattice in two dimensions with lattice spacing a with periodic boundary conditions. The periodic domain is assumed to be a square domain of $N \times N$ lattice sites. The atoms are connected by Hookean springs between nearest and next-nearest neighbors with spring constants K_L and K_D, respectively. For simplicity and easy of calculation the spring constants K_L and K_D are chosen to be independent of the type of bond (Si-Si, Ge-Ge or Ge-Si). However for the Si/Ge system this is a reasonable assumption for the elastic constants for the two species [24]. The displacement of an atom at site (ℓ, j) from the reference configuration is denoted $(u_{\ell,j}, v_{\ell,j})$. Each site on the lattice will be occupied by either a Si or Ge atom (see Fig. 1) and we use the following indicator function to denote the atom type at site (ℓ, j),

$$\theta_{\ell,j} = \begin{cases} 1 & \text{if } (\ell,j) \text{ if site contains a Ge atom} \\ 0 & \text{if } (\ell,j) \text{ if site contains a Si atom.} \end{cases}$$

The equilibrium Si-Si and Ge-Ge bond lengths are denoted as a_s and a_g, whereas the bond length between a Si and a Ge atom is taken to be $\frac{1}{2}(a_s + a_g)$. In this way the relative unstrained bond length between atoms at sites $(\ell + n, j + m)$ and (ℓ, j) is given by

$$f_{\ell+n,j+m} = a_s - a + a_s\mu(\theta_{\ell,j} + \theta_{\ell+n,j+m})/2, \tag{3}$$

where

$$\mu = (a_g - a_s)/a_s. \tag{4}$$

The total elastic energy can then be written as

$$W = W(u, v, \theta) = \frac{1}{2} \sum_{\ell=0}^{N-1} \sum_{j=0}^{N-1} (w^L_{\ell,j} + w^D_{\ell,j}). \tag{5}$$

In this expression, the summand is the total elastic energy in springs connected to the atom at site (ℓ, j) where

$$\begin{aligned} w^L_{\ell j} &= \frac{K_L}{2} \sum_{n\in\{1,-1\}} (\delta u_{\ell+n,j})^2 + (\delta v_{\ell,j+n})^2 \quad \text{and} \\ w^D_{\ell j} &= \frac{K_D}{4} \sum_{n,m\in\{-1,1\}} (n\delta u_{\ell+n,j+m} + m\delta v_{\ell+n,j+m})^2, \end{aligned}$$

and

$$\begin{aligned} \delta u_{\ell+n,j+m} &= u_{\ell+n,j+m} - u_{\ell,j} - f_{\ell+n,j+m} \\ \delta v_{\ell+n,j+m} &= v_{\ell+n,j+m} - v_{\ell,j} - f_{\ell+n,j+m}. \end{aligned}$$

The model we choose is simple enough to be tractable but with the ability to incorporate the discrete nature of the alloy, and to account for the microscopic arrangement of the atoms in an alloy. In most models it is typically assumed that the alloy remains in mechanical equilibrium as it evolves. This means that we need to evaluate the elastic energy, W, when the system is in mechanical equilibrium. The equilibrium displacement field satisfies

$$\frac{\partial W}{\partial u_{\ell,j}} = 0 \quad \text{and} \quad \frac{\partial W}{\partial v_{\ell,j}} = 0.$$

In other words

$$\begin{aligned} & 2K_L(u_{\ell+1,j} - 2u_{\ell,j} + u_{\ell-1,j}) \\ + \;& K_D(u_{\ell+1,j+1} + u_{\ell-1,j+1} + u_{\ell+1,j-1} + u_{\ell-1,j-1} - 4u_{\ell,j}) \\ + \;& K_D(v_{\ell+1,j+1} + v_{\ell-1,j-1} - v_{\ell+1,j-1} - v_{\ell-1,j+1}) \\ = \;& \mu a_s \left[K_L(\theta_{\ell+1,j} - \theta_{\ell-1,j}) + K_D(\theta_{\ell+1,j+1} + \theta_{\ell+1,j-1} - \theta_{\ell-1,j+1} - \theta_{\ell-1,j-1})\right] \end{aligned} \tag{6}$$

and

$$\begin{aligned} & 2K_L(v_{\ell,j+1} - 2v_{\ell,j} + v_{\ell,j-1}) \\ + \;& K_D(v_{\ell+1,j+1} + v_{\ell-1,j+1} + v_{\ell+1,j-1} + v_{\ell-1,j-1} - 4v_{\ell,j}) \\ + \;& K_D(u_{\ell+1,j+1} + u_{\ell-1,j-1} - u_{\ell+1,j-1} - u_{\ell-1,j+1}) \\ = \;& \mu a_s \left[K_L(\theta_{\ell,j+1} - \theta_{\ell,j-1}) + K_D(\theta_{\ell+1,j+1} + \theta_{\ell-1,j+1} - \theta_{\ell+1,j-1} - \theta_{\ell-1,j-1})\right]. \end{aligned} \tag{7}$$

It is easy to see from Eq. (5) that $\dfrac{\partial^2 W}{\partial u^2_{\ell,j}}, \dfrac{\partial^2 W}{\partial v^2_{\ell,j}} > 0$ and $W \to \infty$ as $u_{\ell,j}, v_{\ell,j} \to \pm\infty$ hence the solution to Eq. (6) and Eq. (7) is the unique minimizer of the W. Later in this paper we shall evaluate W when the displacement field satisfies Eqs. (6) and (7). However, now it is useful to look at the continuum limit of these equations.

III. CONTINUUM LIMIT

For alloys, θ can vary on the scale of the lattice and cannot be used as a continuum variable. Instead we appeal to a coarse-grained value:

$$\bar{\theta}_{\ell,j} = \sum_{\ell',j'} A_R(\ell - \ell', j - j')\theta_{\ell',j'} \quad \text{with} \quad \sum_{\ell',j'} A_R = 1$$

where A_R is an averaging kernel and R is a length scale over which the averaging takes place (e.g. $A_R(\ell, j) = C \exp[-(\ell^2 + j^2)/R^2]$ where $C^{-1} = \sum_{\ell,j} \exp[-(\ell^2 + j^2)/R^2]$). Since the coarse-grained variables are smooth functions of of the lattice site, we can introduce a smooth function Θ such that $\bar{\theta}_{\ell,j} = \Theta(a\ell, aj)$.

A. The Displacement Field

We apply the coarse-graining operation to the equations governing the displacement field (i.e. Eqs. (6) and (7)). Since the equations of mechanical equilibrium are linear, it is clear that the coarse-grained variables, $(\bar{u}_{\ell,j}, \bar{v}_{\ell,j})$ satisfy the same equations as the atomistic system. However, unlike their atomistic counterparts the coarse grained variables vary slowly over atomistic scales such that $\bar{u}_{\ell,j} = U(a\ell, aj)$ and $\bar{v}_{\ell,j} = V(a\ell, aj)$, where U and V are smooth functions. We can consequently make use of approximations such as

$$\bar{u}_{\ell+1,j} - 2\bar{u}_{\ell,j} + \bar{u}_{\ell-1,j} \approx a^2 U_{xx}$$

to find that continuum variables satisfy the following equations

$$\begin{aligned} K_L U_{xx} + K_D(U_{xx} + U_{yy} + 2V_{xy}) &= (a_g - a_s)(2K_D + K_L)\Theta_x, \\ K_L V_{yy} + K_D(V_{xx} + V_{yy} + 2U_{xy}) &= (a_g - a_s)(2K_D + K_L)\Theta_y. \end{aligned} \tag{8}$$

Therefore, continuum theory can predict the coarse-grained displacement field in terms of the coarse-grained concentration field. Finally, we point out that for the case $K_L = 2K_D$ the system (8) corresponds to isotropic elasticity. This is seen by noting that the above equations represent the constitutive relation between the stress and the strain and collecting the elasticity tensor (see [10, 25]).

B. Continuum Elastic Energy

The elastic energy is a quadratic function of the displacement field and accordingly it is not a simple matter to apply the coarse-graining operation to W and express the result in terms of the coarse grained variables. Instead, what can be done is to use approximations such as

$$\theta_{\ell+1,j} - \theta_{\ell,j} \approx a\Theta_x \tag{9}$$

and replace the atomistic value of θ by its continuum value, Θ. Given that the atomistic values are not necessarily smooth functions of the lattice site, approximations of the type given by (9) could be rather poor.

Nevertheless, if we apply this procedure to the atomistic energy (Eq. 5), we arrive at the following continuum version of the elastic energy :

$$W_C = \frac{1}{2}\int \left[\, (K_D + K_L)(S_{xx}^2 + S_{yy}^2) + 2K_D S_{xx} S_{yy} + 4K_D S_{xy}^2 \,\right] dxdy, \tag{10}$$

where $S = E - E^0$,

$$E_{jk} = \frac{1}{2}\left(\frac{\partial U_j}{\partial x_k} + \frac{\partial U_k}{\partial x_j}\right)$$

and

$$E^0 = \frac{1}{a}\begin{pmatrix} a_s - a + (a_g - a_s)\Theta & 0 \\ 0 & a_s - a + (a_g - a_s)\Theta \end{pmatrix}.$$

We remark that E^0 is sometimes called the stress free strain. It should be emphasized that Eq. (10) is a commonly used model (e.g. Refs. [5–7]). In addition, the Euler-Lagrange equations for W_C give rise to the equations for continuum elasticity (8). By this we mean

$$\delta W_C = 0 \quad \Rightarrow \quad \sum_{k=1}^{2} \frac{\partial}{\partial x_k}\frac{\partial W_C}{\partial U_{j,k}} = 0$$

will yield (8).

By following the same approach as Cahn [9], we will compute the elastic energy of an alloy in mechanical equilibrium for the isotropic case ($K_L = 2K_D$). We consider a periodic region of size $2\pi \times 2\pi$ and we find

$$W_C = \overline{W} + \widetilde{W}_C,$$

where

$$\overline{W} = 4K_D(a_s - a + \Theta_0(a_g - a_s))^2(2\pi)^2/a^2,$$

and

$$\widetilde{W}_C = \frac{4}{3}K_D\left(\frac{\mu a_s}{a}\right)^2 \int\int (\Theta(x,y) - \Theta_0)^2\, dxdy$$

where Θ_0 = average value of Θ. We note that $\overline{W}$ is the "DC" contribution (Direct Current or non-oscillating) to W_C and $\widetilde{W}_C$ is the contribution from the compositional variations. Notice that by adjusting the lattice spacing a of the reference configuration we can make $\overline{W} = 0$. This value is $a = a_s + \Theta_0(a_g - a_s)$ and is sometimes called Vegard's Law. An important conclusion from this continuum formulation is that the elastic energy is zero for a homogenous alloy whose reference lattice spacing satisfies Vegard's Law.

IV. ELASTIC ENERGY IN THE ATOMISTIC CASE

It should be pointed out that here we are closely following the calculations of Cahn [9]. In this section we apply his approach to discrete equations while he considered continuum equations.

Since we are in the periodic setting it is useful to expand various quantities in a discrete Fourier series. For example

$$\theta_{\ell,j} = \frac{1}{N^2}\sum_{n=0}^{N-1}\sum_{m=0}^{N-1} \hat{\theta}_{m,n} e^{i\alpha(m\ell+nj)} \tag{11}$$

where $\alpha = 2\pi/N$ and $\hat{\theta}_{m,n}$ is the discrete Fourier transform of $\theta_{\ell,j}$. Furthermore, we will for now restrict our calculations to the case $K_L = 2K_D$, in which case the continuum limit is isotropic. Applying the discrete Fourier transform to (6) and (7) and solving for the transformed displacement field we find

$$\hat{u}_{m,n} = \begin{cases} 0 & n = m = 0 \\ \dfrac{-2\mu a_s i\hat{\theta}_{m,n}\cos^2(n\alpha/2)\sin(m\alpha)}{4 - \cos(m\alpha) - \cos(n\alpha) - 2\cos(m\alpha)\cos(n\alpha)} & \text{otherwise} \end{cases} \tag{12}$$

and

$$\hat{v}_{m,n} = \begin{cases} 0 & n = m = 0 \\ \dfrac{-2\mu a_s i\hat{\theta}_{m,n}\cos^2(m\alpha/2)\sin(n\alpha)}{4 - \cos(m\alpha) - \cos(n\alpha) - 2\cos(m\alpha)\cos(n\alpha)} & \text{otherwise,} \end{cases} \tag{13}$$

where $\hat{u}_{m,n}$ and $\hat{v}_{m,n}$ are the discrete Fourier transforms of $u_{\ell,j}$ and $v_{\ell,j}$, respectively.

Our goal is now to calculate the total elastic energy of the ball and spring model when the system is in mechanical equilibrium. To that end, it is useful to define the average value of θ :

$$\theta_0 = \sum_{\substack{n=0 \\ (m,n)\neq(0,0)}}^{N-1}\sum_{m=0}^{N-1} \theta_{m,n}.$$

Now it is worth noting that $\theta_0 = \hat{\theta}_{0,0}$. In view of the two formulas above (12) and (13) it is apparent that each component of the displacement field has mean zero. Therefore, in mechanical equilibrium we have

$$W(u,v,\theta) = W(0,0,\theta_0) + W(u,v,\theta-\theta_0) \equiv \overline{W} + \widetilde{W}$$

where $\overline{W} = N^2 4K_D(a_s - a + \theta_0(a_g - a_s))^2$. The first term, $\overline{W}$, represents the contribution to the elastic energy if the material was of a uniform concentration. The second term, $\widetilde{W}$, results from the compositional variations. We compute $\widetilde{W}$ using Parseval's formula combined with (12) and (13). A lengthy calculation reveals

$$\widetilde{W} = \frac{K_D(a_s\mu)^2}{N^2} \sum_{\substack{n=0 \\ (m,n)\neq(0,0)}}^{N-1} \sum_{m=0}^{N-1} G(\alpha m, \alpha n)|\hat{\theta}_{m,n}|^2 \tag{14}$$

where

$$G(x,y) = \frac{T(x,y)}{8(4 - \cos x - \cos y - 2\cos x \cos y)^2}$$

and

$$\begin{aligned} T(x,y) &= 196 - 87[\cos x + \cos y] + 4[\cos 2x + \cos 2y] + \cos 3x + \cos 3y \\ &- 42[\cos(x-y) + \cos(x+y)] + 2[\cos(2x+2y) + \cos(2x-2y)] \\ &+ 11[\cos(2x+y) + \cos(x+2y) + \cos(2x-y) + \cos(x-2y)] \\ &+ \cos(x-3y) + \cos(3x-y) + \cos(x+3y) + \cos(3x+y). \end{aligned}$$

Since $G(2\pi - k_x, k_y) = G(k_x, 2\pi - k_y) = G(2\pi - k_x, 2\pi - k_y) = G(k_x, k_y)$ it is enough to consider $G(k_x, k_y)$ for $0 < k_x \leq \pi$ and $0 < k_y \leq \pi$.

Notice that $\widetilde{W}$ does not depend on a but $\overline{W}$ does. In fact we can relax our alloy by changing a: If we pick $a = a_s(1 + \theta_0\mu)$ (Vegard's law), then $\overline{W} = 0$. For the remainder this value of a will be used. Therefore the elastic energy of the relaxed alloy is $\widetilde{W}$.

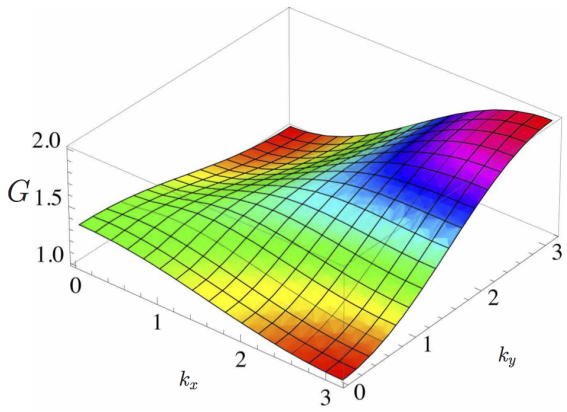

FIG. 2: (Color Online) A plot of $G(k_x, k_y)$ for the case $K_L = 2K_D$ ($K_D = 1$)

The dependence of $\widetilde{W}$ on θ can be gleaned from Fig. 2. Note that $\widetilde{W}$ is a weighted sum of the $G(k_x, k_y)$ with weights $|\hat{\theta}|^2$. Different regions of the k-space represent different aspects of composition profiles. For example, an alloy that is finely intermixed on an atomic scale has weights $|\hat{\theta}|^2$ concentrated near $(k_x, k_y) = (\pi, \pi)$, while for an alloy with variations on continuum length scales the weights are concentrated near $(k_x, k_y) = (0, 0)$. It therefore follows from Fig. 2 that finely mixed alloys have more elastic energy than those that are segregated. Moving along from (π, π) to $(0, 0)$ corresponds to a coarsening patterns with checker board symmetry. The fact that $G(\pi, \pi)/G(0, 0) = 3/2$ indicates that intermixing can significantly increase the elastic energy. Interestingly, it also follows that fine line patterns (along $k_x = 0$ or $k_y = 0$ axis) have even less elastic energy for the case where the constants K_L and K_D are related by $K_L = 2K_D$. Although these

cases can be viewed as different regions of k-space, typical composition profiles would of course have weights in all regions and no separation of scales. Thus, Fig. 2 also points to the difficulty relying on formulas like Eq. (2), since it is clear that the elastic energy depends on the details of the atomistic arrangement over the full range of length scales.

As mentioned above, the behavior near $(k_x, k_y) = (0, 0)$ describes an alloy with variations on continuum length scales and we note that

$$G(\alpha x, \alpha y) = \frac{4}{3} + \frac{3x^4 - 10x^2y^2 + 3y^4}{9(x^2 + y^2)}\alpha^2 + O(\alpha^4), \tag{15}$$

which means the limit $\lim_{(k_x,k_y)\to(0,0)} G(k_x, k_y)$ is well defined and equal to $\frac{4}{3}$. This is consistent with the assertion that the case $K_L = 2K_D$ recovers isotropic elasticity. Furthermore if it assumed that $\theta_{\ell,j}$ is a continuum variable (i.e. $|\hat{\theta}_{m,n}|$ is strongly concentrated at the origin), then

$$\begin{aligned} \lim_{\alpha\to 0} \widetilde{W} &= \frac{4k_D(a_s\mu)^2}{3N^2} \sum_{\substack{n=0 \\ (m,n)\neq(0,0)}}^{N-1} \sum_{m=0}^{N-1} |\hat{\theta}_{m,n}|^2 \\ &= \frac{4}{3} k_D(a_s\mu)^2 \sum_{\ell=0}^{N-1} \sum_{j=0}^{N-1} (\theta_{\ell,j} - \theta_0)^2. \end{aligned} \tag{16}$$

Therefore, the model is anisotropic on small scales and isotropic on large scales. The anisotropy of ball and spring models on atomistic scales has been discussed in Refs. [17, 26].

A. Anisotropic Continuum Limit

We note that for $K_L \neq 2K_D$ the continuum limit becomes anisotropic. It is well known (see [10] page 1447) that in this case the function $G(k_x, k_y)$ is a homogeneous function of order 0 near the origin and $\lim_{(k_x,k_y)\to(0,0)} G(k_x, k_y)$ is not well defined giving rise to the cusp-like behavior near the origin (see Figures 3 and 4).

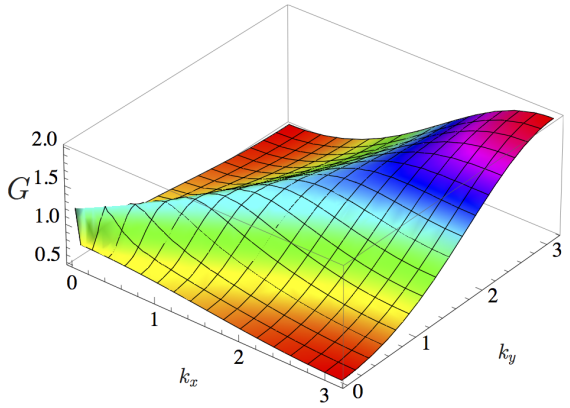

FIG. 3: (Color Online) A plot of $G(k_x, k_y)$ for $K_L = K_D = 1$

The nature of G makes it difficult to make claims about the relative amount of elastic energy in the different scales for a wide range of values of K_L and K_D. However, the behavior along the diagonal is relatively robust, as can be seen in Figure 5. In addition, we can establish that for arbitrary K_L and K_D one has $\lim_{\alpha\to 0} G(\pi, \pi)/G(\alpha, \alpha) = (K_L + 4K_D)/(K_L + 2K_D) > 1$, which suggests that the tendency for a finely mixed systems to have a greater elastic energy than a segregated one persists.

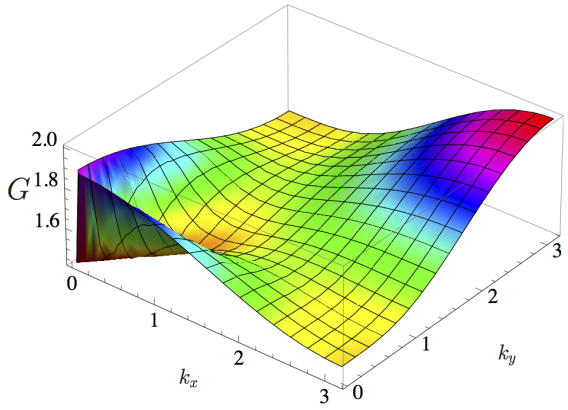

FIG. 4: (Color Online) A plot of $G(k_x, k_y)$ for $K_L = 3K_D$ $(K_D = 1)$

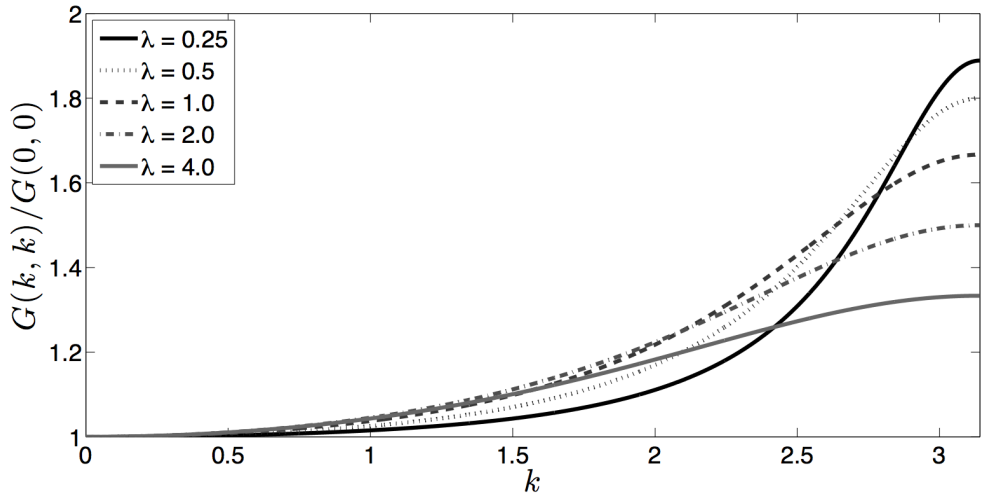

FIG. 5: (Color Online) A plot of $G(k,k)/G(0,0)$ vs k for different values of $\lambda = K_L/K_D$

B. Elastic Enthalpy of Mixing

If we compare Eqs. (14) and (16), it is evident that if one ignores the microscopic scales of the concentration field (i.e. by only considering the Fourier modes near the origin) then the discrete elastic energy is consistent with the continuum elastic energy. But more importantly the discrete and continuum cases are different because the continuum elastic energy fails to account for the contribution of the microscopic scales. The reason the coarse grained displacement field does not suffer from this fate is that the microscopic strain fields average out. Since the energy is a quadratic quantity, the microscopic contributions do not cancel when averaged.

As can be inferred by Tsao [8], atomistic variations of the alloy concentration lead to microscopic strain whose contribution to the elastic energy can be referred to as the elastic contribution to the enthalpy of mixing, H. Therefore, it follows from Eq. (14) that H is determined by both the direction and wavelength of the Fourier modes of the microscopic concentration field. Furthermore, it appears that H cannot be a function of the average concentration unless some simplifying approximations are made. This can be done in one setting, namely if one assumes that the alloy is in local thermodynamic equilibrium. In this case one has, in principle, $H = H(\Theta, T)$. However, when the alloy is not in

local thermodynamic equilibrium, as is the case in epitaxial growth or spinodal decomposition, then $H \neq H(\Theta, T)$, and then H will be determined by details at the atomistic scale. Unfortunately this information is completely lost during coarse graining. This points to the difficulty of modeling elastic energy using continuum theory.

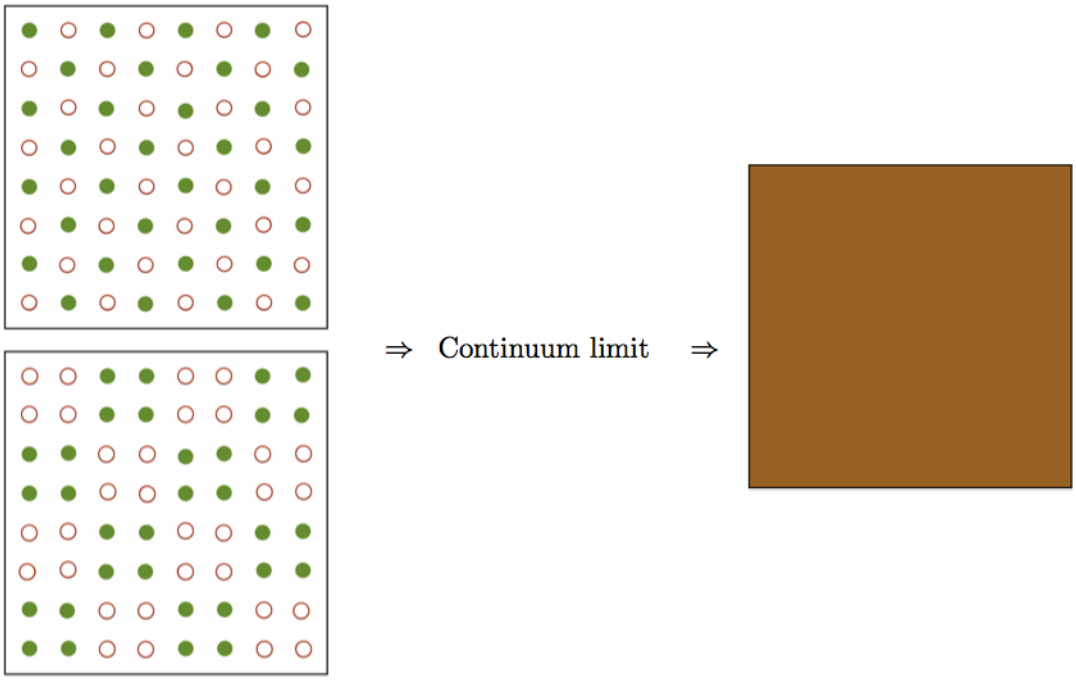

FIG. 6: (Color Online) The figure on the left shows two microscopic arrangements that yield the same continuum alloy concentration (shown on the right). The upper left hand figure shows a 1×1 checkerboard pattern whereas the lower one is a 2×2 pattern.

The following example is useful in elucidating some of the issues discussed above. Consider a binary alloy arranged on a checker board pattern as shown in Fig. 6 ($\theta_{\ell,j} = \frac{1}{2}(1 - (-1)^{\ell+j})$). We have chosen the lattice spacing of the reference configuration to be in accordance with Vegard's Law ($a = \frac{1}{2}(a_s + a_g)$). Clearly then on a continuum scale the alloy can be considered homogeneous $\Theta(x, y) = \Theta_0$ with $\Theta_0 = \frac{1}{2}$. Consequently, the widely used continuum formulation (Eq. 1) predicts that the elastic energy is zero. On the other hand, it is clear that there will be elastic energy in the bonds due to fact that the atoms on this lattice do not correspond to their equilibrium bond length. The continuum approximation ignores the microscopic stress fields. This is fine for the coarse-grained displacement field as the microscopic fields average out. However, when computing the energy the microscopic fields do not average out.

Now one could of course assert that the energy associated with the microscopic strain, calculated above as $\widetilde{W}$ in Eq. (14) is the enthalpic component H of the elastic energy and in many respects it is. However, we will now argue that it cannot be simply characterized by the continuum value of the concentration. This can be seen as follows: Suppose we now coarsen the checker board (see Fig. 6) so that the length scale is 2 atomistic units. Clearly on the continuum scale the alloy can still be considered homogeneous and (Eq. 1) still predicts that the elastic energy is zero. However, if we appeal to Fig. 2 we can infer that the elastic energy of the 2×2 checker board will be smaller than that of the 1×1 checker board, but the continuum value of the alloy concentration has not changed. Therefore, we conclude that the elastic mixing enthalpy of a binary alloy cannot be characterized in terms of the alloy concentration alone. Of course Fig. 2 makes this quite clear.

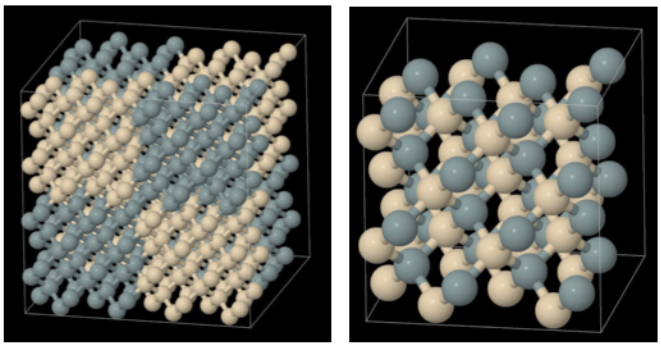

FIG. 7: (Color Online) The atom arrangements for the density functional calculations. The figure on the right shows the $N_C = 1$ checkerboard pattern whereas the one on the left shows the $N_C = 64$ pattern

V. DENSITY FUNCTIONAL THEORY

To explore the broader applicability of the ideas discussed above, we perform DFT calculations for Ge/Si (with a zinc-blende lattice). All results presented here were obtained with the FHI-AIMS code [27]. This is an all-electron full potential DFT code that uses numeric atom centered orbitals as its basis set. We have carefully tested convergence of our results with respect to the basis set, and the density of the (numerical) integration mesh, and have used parameters as they are implemented in FHI-AIMS in the default setting "tight" [27]. We use GGA-PBE for the exchange-correlation functional [28]. All calculations were done with supercells with periodic boundary conditions, and the geometric configurations are fully relaxed.

Before we discuss the DFT results we note that one cannot simply repeat the calculation done in the case of the ball and spring model. The reason is that DFT provides one with the total energy for a given configuration, which has no clear separation between bond and elastic energy. However, for Si or Ge bulk and Si-Ge in a perfect unstrained lattice the only contribution to the energy is the chemical bond energy. If we assume that each atom forms exactly 4 bonds with its nearest neighbors (which is reasonable for a zinc-blende structure), we can estimate the Si-Si, Ge-Ge, and Si-Ge bond-strengths $E^B_{\rm Si}$, $E^B_{\rm Ge}$, and $E^B_{\rm SiGe}$ as follows: We calculate the energy of a bulk system with N_{total} atoms, subtract the energy of N_{total} isolated atoms, and divide this number by $2N_{total}$. In a strained system, the elastic contribution $E^{\rm el}$ is defined as the difference between the total energy of the strained system and the sum of all nearest neighbor bonds. This definition of $E^{\rm el}$ is consistent with assuming that during the mechanical relaxation the bond energy remains the same while the elastic energy changes and that the total energy is the sum of elastic and bond energies. All of our calculations are at $T = 0$, so there are no entropic contributions.

TABLE I: Bond strengths E^B (in eV) calculated with DFT.

lattice constant	$E^B_{\rm Si}$	$E^B_{\rm Ge}$	$E^B_{\rm SiGe}$	$\frac{1}{2}(E^B_{\rm Si} + E^B_{\rm Ge})$
$a_{\rm Si}$	2.677	2.176	2.431	2.426
$a_{\rm SiGe}$	2.661	2.213	2.442	2.437
$a_{\rm Ge}$	2.608	2.227	2.420	2.418

We calculated the bond energies for systems where all atoms are in a lattice with the optimized lattice constants $a_{\rm Si}$, $a_{\rm Ge}$, and $a_{\rm SiGe}$. The optimized lattice constants are calculated by optimizing three different configurations. The first consists purely of Si atoms. The second purely of Ge atoms. The third system used to calculate $a_{\rm SiGe}$ consists of 50% Si and 50 % Ge arranged in an alternating fashion so that all bonds in the zinc blend structure are Si-Ge bonds and are configurationally equivalent to one another under periodic boundary conditions. Thus the uniform lattice spacing of the optimized structure yields the $a_{\rm SiGe}$ lattice spacing. The three different bond strengths are calculated in a similar manner. The results are shown in table I. For all lattice constants we find

that $E^B_{\rm Si}$ is stronger than $E^B_{\rm Ge}$, while $E^B_{\rm SiGe}$ is in-between. But a closer inspection of the numbers reveals that $E^B_{\rm SiGe}$ is 2 to 5 meV stronger than the average of $E^B_{\rm Si}$ and $E^B_{\rm Ge}$ for all lattice constants. This implies that simple bond counting arguments predict that a perfectly intermixed Si/Ge system is always preferred, regardless of whether the system has the lattice constant $a_{\rm SiGe}$, is compressed to $a_{\rm Si}$, or is stretched to $a_{\rm Ge}$.

Now we proceed to understand the system with elastic effects. For this we consider various configurations of a $Si_{0.5}Ge_{0.5}$ alloy. We compare bulk alloy composition profiles that resemble a 3-dimensional checkerboard, where each "checker-unit" consists of 1, 8, or 64 atoms of the same type (i.e., all Si or all Ge) occupying a cubic region in space (see Fig. 2). This corresponds to moving along the diagonal for G (cf. Fig. 2). We do this by placing the configuration in a zinc blend lattice with reference lattice constant $a_{\rm Si}$ or $a_{\rm SiGe}$ and then optimizing the structure.

Table II summarizes the DFT results. $\Delta E^{\rm tot}$ is the difference in the total energy ($E^{\rm tot}$ that includes bond and elastic energies) for systems with checker units that consist of N_C atoms, and a checkerboard with $N_C = 1$. For a system with the lattice constant $a_{\rm Si}$ (which is most relevant for Ge deposition on Si) we find that the checkerboard with $N_C = 8$ is preferred by 1 meV per atom (over a system with $N_C = 1$), and that one with $N_C = 64$ is preferred by 4 meV per atom. For the lattice constant $a_{\rm SiGe}$, the coarser system with $N_C = 64$ is also preferred, but only by 1 meV.

The numbers for $\Delta E^{\rm el}(N_C) = E^{\rm el}(N_C) - E^{\rm el}(N_C = 1)$ represent the change in energy per atom after correcting for the fact that simple bond counting arguments favor intermixing and should be considered the true elastic contribution due to coarsening. For example, for a system with $N_C = 8$, half of the bonds are converted from being Si-Ge bonds to being either Si-Si or Ge-Ge bonds, and one can show that $\Delta E^{\rm el} = \Delta E^{\rm tot} - 1/2E^B_{\rm Si} - 1/2E^B_{\rm Ge} + E^B_{\rm SiGe}$. Since the average of the Si-Si and Ge-Ge bond is 5 meV weaker than the Si-Ge bond (cf. table I), intermixing is preferred by 5 meV per atom for this system. Similarly, for a system with $N_C = 64$, $\Delta E^{\rm el} = \Delta E^{\rm tot} - 2/3E^B_{\rm Si} - 2/3E^B_{\rm Ge} + 4/3E^B_{\rm SiGe}$, and intermixing is preferred by 7 meV per atom. $\Delta E^{\rm el}$ then represents the fact that elastic contributions have to overcome this favoring of intermixing. The results confirm that elastic effects favor segregation.

We further note that the numbers given in table I and II are real numbers. The units are in eV. The accuracy of the DFT calculations is at best of the order of meV. Therefore, we have rounded the results to 3 significant digits past the decimal point (i.e., meV). In table II we then report differences, and these are given in meV.

TABLE II: $\Delta E^{\rm tot}$ and $\Delta E^{\rm el}$ for different values of N_C. Energy changes (in meV) are with respect to a system with $N_C = 1$ (a perfect zinc-blende structure).

N_C	$\Delta E^{\rm tot}(a_{\rm Si})$	$\Delta E^{\rm tot}(a_{\rm SiGe})$	$\Delta E^{\rm el}(a_{\rm Si})$	$\Delta E^{\rm el}(a_{\rm SiGe})$
1	0	0		
8	-1	1	-6	-4
64	-4	-1	-11	-8

In addition we have done DFT calculations where we considered $Si_{0.5}Ge_{0.5}$ systems with alternating layers of Si and Ge. These layers are periodic in 2 dimensions and have layer thicknesses 1 and 2. The layers are oriented along the (100) direction, and consist of a bi-layer of Si and Ge. For these systems we also find that a thicker layer is preferred by 1 meV (2 meV) when the system has the lattice constant $a_{\rm Si}$ ($a_{\rm SiGe}$). This trend continues for thicker layers (but additional changes are less pronounced).

VI. HETEROEPITAXIAL THIN FILMS

We now consider a strained flat film of thickness T of pure Ge on a semi-infinite substrate of pure Si. This case has a free surface unlike the periodic cases discussed above. According to continuum theory, the total elastic energy will be

$$W = C\mu^2 AT,$$

where C depends on the elastic properties and A is the area of the film. Now suppose that Si and Ge mix perfectly in such a way that the film has a fraction θ_0 of Ge. The film now has a thickness T/θ_0 and an effective misfit of $\mu(\theta_0) = \theta_0\mu$ [7]. By continuum theory the total elastic energy is

FIG. 8: (Color Online) The eight atom checker board pattern. There are 64 (8×8) atoms in each checker board.

TABLE III: Normalized Total elastic energy

1 atom checker board	1.241
2 atom checker board	1.050
4 atom checker board	0.976
8 atom checker board	0.947
random arrangement	1.012
continuum theory	0.500

Therefore, according to continuum theory, the total elastic energy is reduced by intermixing. In view of the previous discussion this is not expected to be true for the ball and spring model. To that end, we performed a numerical calculation using the method in Ref. [29] to calculate the elastic energy of the ball and spring with $K_L = 2K_D$ and $\mu = .04$. The film is 40 monolayers thick and consists of an equal number of Si and Ge atoms. We considered 4 cases in which the atoms are arranged in checker board patterns, where the only difference is that the scale of the pattern changes. On the finest scale, each square consists of exactly one atom. For a reference state we computed the total elastic energy of a thin film with 20 monolayers of pure Ge on a substrate of pure Si. Note that the total number of Ge atoms is the same in each of the 4 cases and in the reference state. We note that the reference configuration corresponds to $\theta_0 = 1$ with a film thickness of 20 layers and all the checker board patterns in the continuum model are equivalent to $\theta_0 = 0.5$ with a film thickness of 40 layers. The normalized elastic energy is the total elastic energy divided by the elastic energy of the reference state. The results are summarized in table III. As noted above for the continuum theory the reference configuration has lower elastic energy. However when microscopic segregation is accounted for in the discrete elastic model a segregated configuration is seen to lower elastic energy over both the reference state and a random mixture of $\theta_0 = 0.5$ (the continuum equivalent). It is in particular worth noting that the elastic energy predicted for the continuum case is a factor of two smaller than the discrete case. This is due to the fact that the discrete alloys have longitudinal variations in the concentration profile and hence have an induced strain field in the substrate that decays slowly. This slow decay of the strain field particularly in the case of random mixtures was observed previously in [29] for the ball and spring model. The homogeneous continuum case however has zero strain in the substrate leading to a significantly lower elastic energy in comparison to the random mixture.

It is also clear that the total elastic energy significantly increases as the length scale of the pattern decreases. This indicates that intermixing actually increases the elastic energy for this ball and spring model in the setting of strain thin films.

VII. CONCLUSIONS

We have considered the behavior of the elastic energy of the binary alloys using both an atomistic model (ball and spring) and density-functional theory. Our ball and spring calculation indicates that finely mixed alloys have more elastic energy than those that are more coarsely mixed. This is due to the presence of microscopic strain. The more finely mixed the alloy becomes the more difficult it is for it to elastically relax (the system is frustrated). The important consequence of these observations is that intermixing will actually increase the strain energy of alloy and not lower it as predicted by continuum theories without enthalpic contributions. One may speculate that this is an artifact of the ball and spring model but calculations with DFT support our conclusions.

We mention that some of the difficulties faced using continuum models can be somewhat mitigated by including an elastic component to the enthalpy of mixing. However, this would be quite challenging since we have shown that the elastic energy of an alloy is in fact dependent on the microscopic rearrangements of the atoms – information typically lost in continuum models. In many applications the atomic arrangement is constantly changing both its scale and the degree of anisotropy, making it difficult to assess the elastic energy in terms of average values of the composition. Simply put, the elastic energy of a material cannot be determined by the alloy concentration alone - much more information is needed. One possibility currently being explored is the use of something like an H-measure but with length scale information.

Acknowledgments

We gratefully acknowledge conversations with J.M. Millunchick, V. Shenoy, J. Tersoff, and P. Voorhees. This research was supported, in part, by NSF grants DMS-0810113, DMS-0854870, DMS-1115252, and DMS-0439872.

[1] V.A. Shchukin and D. Bimberg, Spontaneous ordering of nanostructures on crystal surfaces, *Rev. Mod. Phys* **71**, 1125-1171 (1999).
[2] H.Y. Hwang, Y. Iwasa, M. Kawasaki, B. Keimer, N. Nagaosa, and T. Tokura, Emergent phenomena at oxide interfaces, *Nature Materials* **11**, 103 (2012).
[3] J. Yang, A. Sudik, C. Wolverton, and D.J. Siegel, High capacity hydrogen storage materials: attributes for automotive applications and techniques for materials discovery *Chemical Society Reviews* **39**, 656 (2009).
[4] Y.-W. Mo, D.E. Savage, B.S. Swartzentruber, and M.G. Lagally, Kinetic pathway in Stranski-Krastanov growth of Ge on Si(001), *Phys. Rev. Lett.* **65**, 1020 (1990).
[5] B.J. Spencer, P.W. Voorhees, and J. Tersoff, Morphological instability theory for strained alloy film growth: The effect of compositional stresses and species-dependent surface mobilities on ripple formation during epitaxial film deposition, *Phys. Rev. B* **64**, Art. No. 235318 (2001).
[6] Y.H. Tu and J. Tersoff, Origin of apparent critical thickness for island formation in heteroepitaxy, *Phys. Rev. Lett.* **93**, Art. No. 216101 (2004).
[7] N. V. Medhekar, V. Hegadekatte, and V. B. Shenoy, Composition maps in self-assembled alloy quantum dots, *Phys. Rev. Lett.* **100**, 106104 (2008).
[8] J.Y. Tsao, Fundamentals of Molecular Beam Epitaxy, Academic Press, New York, 1993 (see Chapter 4).
[9] J.W. Cahn, On spinodal decomposition, *Acta Metallurgica* **9**, 795-801 (1961).
[10] P. Fratzl, O. Penrose, and J.L. Lebowitz, Modeling of phase separation in alloys with coherent elastic misfit, *J. Stat. Phys.* **95**, 1429-1503 (1999).
[11] L-Q. Chen, Phase-field models for microstructure evolution, *Annual Review of Materials Research* **32**:113-140 (2002).
[12] C. S. Barett, Structure of Materials, McGraw-Hill New York, 1952.
[13] W. Hume-Rothery, R. E. Smallman and C. W. Hayworth, The Structure of Metals and Alloys, The Institute of Metals Monograph and Report Series No. I (1962).
[14] D. de Fontaine, Configurational Thermodynamics of Solid Solutions, *Solid State Physics* **34**, 73-274 (1979).
[15] X.B. Ren, X.T. Wang, K. Shimizu, and T. Tadaki, Effect of elastic energy due to atomic size factor on ordering and decomposition behavior of binary solid solutions, *J. Mater. Sci. Techol.* **12**, 135-142 (1996).

[16] Eshelby, The continuum theory of lattice defects, *Solid State Physics-Advances in Research and Applications* **3**, 79-144 (1956).
[17] H. Cook & D. de Fontaine, On elastic free energy of solid solutions .I. Microscopic theory, *Acta Metallurgica* **17**, 915-924 (1969).
[18] A. G. Khachaturyan, Theory of Structural Transformations in Solids, John Wiley & Sons, New York, (1983).
[19] T. Walther, C. J. Humphreys and A. G. Cullis, Observation of vertical and lateral Ge segregation in thin undulating SiGe layers on Si by electron energy-loss spectroscopy, *Appl. Phys. Lett.* **71**, 809-811 (1997).
[20] W. Hume-Rothery, G.W. Mabbott and K.M.C. Evans, The freezing points, melting points, and solid solubility limits of the alloys of silver and copper with the elements of the B sub-groups, *Phil. Trans. Roy. Soc. London A* **233** 1-97 (1934).
[21] H.W. King, Quantitative Size-Factors for Metallic Solid Solutions, *Journal of Material Science***1**, 79-90 (1966) (see page 83).
[22] J.E. Woodilla Jr. and B.L. Averbach, Modulated Structures in Au-Ni Alloys, *Acta Materialia* **16**, 255-263 (1968).
[23] B. Golding and S.C. Moss, A re-calculation of the gold-nickel spinodal, *Acta Metellurgica* **15** 1239-1241 (1967).
[24] J. J. Wortman and R. A. Evans, Young's Modulus, Shear Modulus, and Poisson's Ratio in Silicon and Germanium, *Journal of Applied Physics* **36** 153 (1965).
[25] T.P. Schulze and P. Smereka, An Energy Localization Principle and its Application to Fast Kinetic Monte Carlo Simulation of Heteroepitaxial Growth, *Journal of the Mechanics and Physics of Solids* **57**, 521 - 538 (2009).
[26] P. Fratzl and O. Penrose, Ising-model for phase-separation in alloys with anisotropic elastic interaction. 1. Theory, *Acta Metallurgica et Materialia* **43** 2921-2930 (1995).
[27] V. Blum, R. Gehrke, F. Hanke, P. Havu, V. Havu, X. Ren, K. Reuter, and M. Scheffler, *Computer Physics Communications* **180** 2175-2196 (2009).
[28] J. P. Perdew, K. Burke, and M. Ernzerhof, Generalized gradient approximation made simple, *Phys. Rev. Lett.* **77**, 3865-3868 (1996).
[29] A. Baskaran, J. Devita and P. Smereka, Kinetic Monte Carlo simulation of strained heteroepitaxial growth with intermixing, *Continuum Mechanics and Thermodynamics* **22**, 26 (2010).